

# Selected Configuration Interaction in a Basis of Cluster State Tensor Products

Vibin Abraham and Nicholas J. Mayhall\*

*Department of Chemistry, Virginia Tech, Blacksburg, VA 24060, USA*

Selected configuration interaction (SCI) methods are currently enjoying a resurgence due to several recent developments which improve either the overall computational efficiency or the compactness of the resulting SCI vector. These recent advances have made it possible to get full CI (FCI) quality results for much larger orbital active spaces, compared to conventional approaches. However, due to the starting assumption that the FCI vector has only a small number of significant Slater determinants, SCI becomes intractable for systems with strong correlation. This paper introduces a method for developing SCI algorithms in a way which exploits local molecular structure to significantly reduce the number of SCI variables. The proposed method is defined by first grouping the orbitals into clusters over which we can define many particle cluster states. We then directly perform the SCI algorithm in a basis of tensor products of cluster states instead of Slater determinants. While the approach is general for arbitrarily defined cluster states, we find significantly improved performance by defining cluster states through a self-consistent Tucker decomposition of the global (and sparse) SCI vector. To demonstrate the potential of this method, called tensor product selected configuration interaction (TPSCI), we present numerical results for a modified Hubbard model with different inter- and intra-cluster hopping terms. We also study the less obviously clusterable cases of bond breaking in  $N_2$  and CO and also singlet-triplet gaps in planar  $\pi$ -conjugated systems. Numerical results show that TPSCI can be used to reduce the number of variables in the variational space quite significantly as compared to other selected CI approaches.

## I. INTRODUCTION

The efficient simulation of strongly correlated electrons remains a key challenge toward better understanding several critical areas of chemical and molecular sciences including catalysis, organometallic chemistry, excited state processes, and many more. Although the term “strongly correlated” is rather ambiguously defined, we will take this to mean a system which cannot be efficiently and accurately modeled using perturbative or diagrammatic techniques starting from a single Slater determinant wavefunction. For systems dominated by one-electron interactions, Hartree-Fock (HF) represents a useful approach, such that the resulting single Slater determinant wavefunctions are qualitatively accurate. Consequently, the full configuration interaction (FCI) wavefunction written as a sum of all possible determinants bears a near unit coefficient weighting the HF ground state determinant. Methods such as perturbation theory, or coupled-cluster work extremely well in this regime. However, as the relative strength of the two-electron component increases, the HF state becomes less useful as an approximation, with many different determinants contributing significantly. This leads to a breakdown of most common approximations, such as perturbation theory, coupled-cluster theory, density functional theory, etc.

Although any algorithm which solves an *arbitrary* strongly correlated system is likely to exhibit exponential scaling, it is often the case that a molecule’s Hamiltonian has some structure that can be exploited to make the problem easier. For example, if a molecule’s strong correlation arises due to an orbital near-degeneracy, then active-space methods are effective in obtaining accurate results from a relatively simple computation. For systems which have a near one-dimensional structure, ma-

trix product states provide highly efficient representations which can be solved for using density matrix renormalization group (DMRG).<sup>1–3</sup> Likewise, approximately two-dimensional structure can be efficiently parameterized using projected entangled pair states (PEPS),<sup>4,5</sup> and recent improvements in contraction algorithms have made these algorithms more promising for molecular applications.<sup>6</sup> More general tensor networks have also been explored.<sup>7–11</sup> For systems whose strong correlation occurs among a relatively small subset of Slater determinants (as opposed to a single particle subset defining an active-space) one might choose to perform a configuration interaction (CI) calculation using only the important Slater determinants. This is the physical motivation for so-called “selected CI” methods which have a long history in the field,<sup>12–14</sup> but which have seen a resurgence during the past few years.<sup>15–21</sup>

Selected CI methods typically involve an iterative procedure in which a CI calculation is performed within a small subspace of Slater determinants, and this subspace is iteratively refined using some search algorithm to find the most important Slater determinants. The basic algorithmic steps of a selected CI program involve:

1. Determine an initial variational space (typically either the HF determinant or the set of single and double excitations).
2. Find the ground state of the Hamiltonian in the current variational space.
3. Perform some search algorithm which identifies which determinants outside of the space are most important. This importance criterion is usually based on perturbative or energy minimization estimates.

4. Construct a new variational space based on the search results, and continue until the spaces stop changing.

Although all selected CI approaches follow these general steps, they differ in various details. As one of the first approaches of this sort, the configuration interaction perturbatively selected iteratively (CIPSI)<sup>12</sup> algorithm builds the CI space by adding determinants which have first order coefficients larger than some threshold,  $\epsilon$ . More recently, the Adaptive Sampling CI (ASCI)<sup>15</sup> method accelerated the CIPSI algorithm by only considering a few determinants with large coefficients in the current model space. In this work, the authors also showed that SCI algorithm is basically a deterministic variant of the FCI-QMC proposed by Booth and coworkers.<sup>22,23</sup> With the goal of achieving better accuracy guarantees, the  $\Lambda$ -CI method adds determinants based on a variational energy criterion  $\Lambda$ .<sup>24</sup> Following their earlier work, Evangelista and co-workers then proposed the adaptive CI (ACI) method which produces compact wavefunctions with tunable accuracy.<sup>16</sup> As a deterministic generalization of heat-bath sampling,<sup>25</sup> heat-bath CI (HCI)<sup>17,26,27</sup> adds determinants based on the magnitude of the Hamiltonian matrix element. This selection criteria is very cost efficient since it avoids sampling the determinants directly by using the magnitude of the integrals themselves, skipping the denominator computation for the selection step. The Monte Carlo CI (MCCI) method, proposed by Greer, repeatedly adds interacting configurations randomly to the reference space and generates a variational space.<sup>28,29</sup>

All of the SCI methods mentioned above succeed when the number of significant coefficients in the FCI wavefunction is small, and they fail when this number becomes large. This becomes problematic when the degree of strong correlation increases. Luckily, the distribution of FCI wavefunction coefficients directly depends on the choice of basis. This presents a natural question: *Can one find a basis (not necessarily comprised of Slater determinants) which yields a more compact FCI wavefunction, thus decreasing the number of variational parameters in a SCI procedure?*

In this paper, we explore a new basis designed to provide a more compact representation of the wavefunction leading to more efficient SCI calculations. This basis is defined by performing many-body rotations on disjoint sets of orbitals (or “clusters”). The resulting tensor product state basis can incorporate a large amount of electron correlation into the basis vectors themselves. As a result, the exact FCI wavefunction written in terms of tensor product states is much more compact, requiring significantly fewer basis vectors than in the analogous expansion in terms of Slater determinants. In the following sections we describe the construction of the tensor product state basis by way of a self-consistent, sparse Tucker decomposition of a global state vector,<sup>30</sup> and our method to exploit the resulting compactness by developing a framework for performing CIPSI calculations di-

rectly in terms of tensor product states. We refer to this method as tensor product selected CI (TPSCI), and we investigate the numerical performance for a number of strongly correlated systems. A cartoon schematic of the TPSCI method is shown in Fig. 1.

## II. THEORY

In this section, we start by providing a description of our notation used to represent arbitrary tensor product states, which is similar to the work by Scuseria and co-workers in their cluster-based mean field study.<sup>31</sup> We then explain how the Hamiltonian matrix elements can be obtained between arbitrary tensor product states and give a layout of the TPSCI algorithm used in this paper. Finally, we discuss the Tucker decomposition technique used to compress the TPSCI wavefunction.

### A. Tensor Product State

We start by partitioning the spatial orbitals into clusters. Within each cluster,  $n$ , we can define a set of cluster states,  $|n_I\rangle$ , each of which is a linear combination of all possible Slater determinants involving a cluster’s orbitals. A global tensor product state (TPS) over the full system can be represented using these cluster states as:

$$|\psi_I\rangle = |1_I\rangle |2_I\rangle \dots |n_I\rangle \quad (1)$$

By taking all possible tensor products of local cluster states (involving all sectors of a cluster’s Fock space), we exactly span the original Hilbert space. Thus, the exact full CI wavefunction can be represented in this TPS basis as

$$|\Psi\rangle = \sum_{1_I} \sum_{2_J} \dots \sum_{n_Z} c_{1_I, 2_J, \dots, n_Z} |1_I\rangle |2_J\rangle \dots |n_Z\rangle \quad (2)$$

Here  $c_{1_I, 2_J, \dots, n_Z}$  is the expansion coefficient in front of the corresponding TPS configuration.

This orbital clustering can be chosen based on orbital locality, symmetry of the system, or any other criterion. While the choice of this clustering is up to the user, the guiding principle is that the Hamiltonian should act more strongly within clusters and more weakly between them. If a reasonable clustering can be found, an accurate approximation to the FCI state can be represented using few tensor product states as compared to the full space.

### B. Matrix Elements

In order to optimize the expansion coefficients of the TPS basis vectors described above, one needs to evaluate the Hamiltonian matrix elements between arbitrary TPS configurations. Although the matrix elements in a

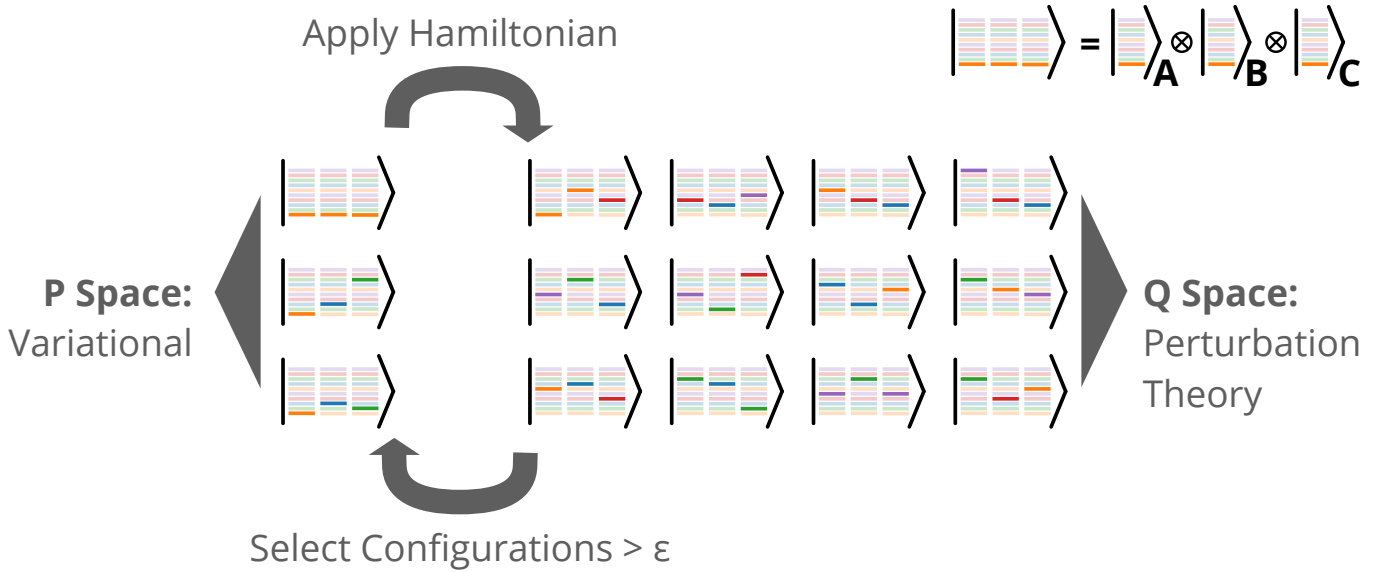


FIG. 1: Schematic representation of the TPSCI algorithm for a three cluster problem. Each stack of lines indicates the different local states for each cluster, with different colors indicating different particle number states. Bold colors indicate that the state is activated in that basis vector. The threshold,  $\epsilon$ , can be used to move states from  $\mathcal{Q}$  to  $\mathcal{P}$ , based on the magnitude of the first order wavefunction (though other criteria could be used as well).

traditional determinant-based CI code are quite straightforward, the TPS matrix elements are significantly more involved.

To start, we first partition the second quantized Hamiltonian,

$$\hat{H} = \sum_{pq} h_{pq} \hat{p}^\dagger \hat{q} + \frac{1}{2} \sum_{pqrs} \langle pq || rs \rangle \hat{p}^\dagger \hat{q}^\dagger \hat{s} \hat{r} \quad (3)$$

into distinct operators which are labelled by the clusters they act upon.

$$\hat{H} = \sum_i \hat{H}_i + \sum_{i,j} \hat{H}_{ij} + \sum_{i,j,k} \hat{H}_{ijk} + \sum_{i,j,k,l} \hat{H}_{ijkl} \quad (4)$$

For instance,  $\hat{H}_i$  corresponds to the operators that are local to cluster,  $i$ . The two-body term  $\hat{H}_{ij}$  involves all Hamiltonian operators such that the operator indices occur in clusters  $i$  and  $j$ . Interactions such as 2-body charge-transfer, exchange, and dispersion fall within this set. The details of implementing the one-body and two-body terms have been worked out by Shiozaki and coworkers as part of the ASD method.<sup>32,33</sup> However, unlike in ASD which is defined for two clusters, we assume an arbitrary number of clusters. As a result, we must also handle the 3-body and 4-body Hamiltonian terms.

Due to the antisymmetric nature of fermions, many of the above “local” terms require a non-local treatment. For instance, to act a creation operator on cluster 3, it must first anticommute through the first two clusters. While a general algorithm can be defined easily when using the Jordan-Wigner spin mapping (and this was the basis for our initial proof of principle code), this approach

incurs significant overhead, and prevents efficient vectorization. Thus in order to simplify the implementation, and speed up the matrix element construction, we make the restriction that each cluster state has well-defined particle number and  $\hat{S}_z$ . In other words, we don’t allow mixing between the local cluster states in different Fock spaces. This also has the added benefit of extra Hamiltonian sparsity and trivial quantum number preservation of the global state determined before doing any numerically intensive tensor contractions.

To provide a concrete example, let us consider one contribution to the two-body matrix element:

$$\hat{H}_{ij} \Leftarrow \sum_{pqr} \sum_s^j \langle pq || rs \rangle \hat{p}^\dagger \hat{q}^\dagger \hat{s} \hat{r} \quad (5)$$

$$= - \sum_{pqr} \sum_s^j \langle pq || rs \rangle \left\{ \hat{p}^\dagger \hat{q}^\dagger \hat{r} \right\} \left\{ \hat{s} \right\} \quad (6)$$

between two arbitrary TPS configurations:

$$|\psi_I\rangle = |1_I\rangle |2_I\rangle \dots |i_I\rangle \dots |j_I\rangle \dots |n_I\rangle \quad (7)$$

$$|\psi_J\rangle = |1_J\rangle |2_J\rangle \dots |i_J\rangle \dots |j_J\rangle \dots |n_J\rangle. \quad (8)$$

Here, we first move each group of operators to the associated cluster it acts on, keeping track of any signs.

$$\sum_{pqr} \sum_s^j \langle pq || rs \rangle \left\{ \hat{p}^\dagger \hat{q}^\dagger \hat{r} \right\} \left\{ \hat{s} \right\} |1_I\rangle \dots |i_I\rangle \dots |j_I\rangle \dots \quad (9)$$

$$= (-1)^x \sum_{pqr} \sum_s^j \langle pq || rs \rangle |1_I\rangle \dots \hat{p}^\dagger \hat{q}^\dagger \hat{r} |i_I\rangle \dots \hat{s} |j_I\rangle \dots \quad (10)$$

where  $\chi = \sum_{k=i}^{j-1} N_K$ , meaning we just sum the number of electrons in each state on clusters between the two active clusters. Next applying the bra to get the matrix element, we are left with:

$$\langle \psi_J | \hat{H}_{ij} | \psi_I \rangle \leftarrow (-1)^\chi \sum_{pqrs} \langle pq || rs \rangle \gamma_{pqr}^{iJ, iI} \gamma_s^{jJ, jI} \quad (11)$$

$$\times \prod_{k \neq i, j} \delta_{k_J, k_I}$$

where the operator tensors,  $\gamma_{pqr}^{jJ, jI} = \langle J | \hat{p}^\dagger \hat{q}^\dagger \hat{r} | I \rangle_j$ , are quantities local to cluster  $j$ . These are similar to transition density matrices, and are precomputed and accessed from memory when needed in the above expressions. The above Kronecker delta indicates that the matrix element between any two TPS configurations is zero, unless all of the non-active cluster states are in the same state. This is the TPS analogy to Slater-Condon rules, and significantly reduces the number of terms we must compute. Similar manipulations are required for all the various 1, 2, 3, and 4 body terms.

### C. TPSCI Algorithm

Once the matrix elements have been implemented, then the exact state can *in principle* be obtained in the TPS basis. However, as described in the introduction, this is intractable, and we need some method for identifying important TPS configurations. To achieve this, we use the SCI strategies developed for Slater determinants and adapt them for generating a compact basis of TPS configurations. While all of the different SCI strategies described above in the introduction could be leveraged in this TPS basis, for this initial report we simply based our work on the earlier CIPSI method. A schematic overview of the TPSCI method is shown in Fig. 1.

The algorithmic steps for TPSCI are quite similar to the Slater determinant CIPSI:

1. **Initialize the variational  $\mathcal{P}$  space.** With Slater determinants, this might be done by choosing either the HF state or CISD space. In this work we initialize by deciding on an initial Fock space configuration which defines how many electrons are in each cluster to begin with. We then choose the lowest energy TPS with that Fock space configuration. Alternatively, one can choose multiple Fock space configurations, and this is sometimes useful when describing delocalized states.
2. **Build the Hamiltonian matrix in the current  $\mathcal{P}$  space and diagonalize.** Although our current code is limited to single thread execution, this step is done matrix element-by-matrix element, and as such, could be perfectly parallelized, reducing the cost of this step immensely. Another point, although our current code builds the full Hamiltonian matrix, this can trivially be adapted to perform a

matrix-vector product to avoid constructing the full matrix. If any variationally obtained configurations fall below a threshold, remove them from  $\mathcal{P}$  space.

3. **Calculate the action of the Hamiltonian on each configuration in the  $\mathcal{P}$  space.** This is the most intricate step of the code, and can easily be improved by only considering the dominant  $\mathcal{P}$  configurations. This is implemented by taking an input TPS and outputting a list of TPS configurations with coefficients. This provides a list of all TPS configurations coupled to the input  $\mathcal{P}$  space via the associated Hamiltonian operator. Before adding the new TPS configurations to our PT space, or  $\mathcal{Q}$  space, we check to make sure the Hamiltonian coefficient is non-zero (or larger than some small threshold). Similar to step 2, this step could also be (but is not yet) trivially parallelized over TPS configurations in the  $\mathcal{P}$  space.
4. **Compute first order coefficients in the  $\mathcal{Q}$  space.** For all configurations in the  $\mathcal{Q}$  space, compute the energy to form an Epstein-Nesbet<sup>34,35</sup> first order energy denominator.

$$C_\alpha = \frac{\sum_i H_{\alpha i} c_i}{E - H_{\alpha\alpha}} \quad (12)$$

Though seemingly a trivial step, this step takes considerable time in our current implementation, and an alternative TPS based HCI approach would be interesting to pursue. This step can also be easily parallelized. Use the first order coefficients to obtain a PT2 correction to the current TPSCI variational energy,

$$\delta E_{PT2} = \sum_\alpha \frac{|\langle \psi | H | D_\alpha \rangle|^2}{H_{\alpha\alpha} - E} \quad (13)$$

and add all  $\mathcal{Q}$  space configurations with coefficients larger than  $\epsilon$  to the  $\mathcal{P}$  space. If no new configurations are above  $\epsilon$ , then the algorithm is finished. Otherwise go to step 2.

### D. Tucker Decomposition

Up to this point, we have yet specified the nature of the cluster states. One naive choice would be to just use the eigenvectors obtained by diagonalizing the local Hamiltonians (the operators which have all indices within a cluster). However, similar to the motivation for DMRG, this basis often does not lead to sufficiently compact representations. If only two clusters are present, then an SVD of the global state could be performed which would provide a maximally compact representation. When considering systems with multiple clusters, no such unique and optimal decomposition exists. However, we can still use the same physical intuition and define the cluster

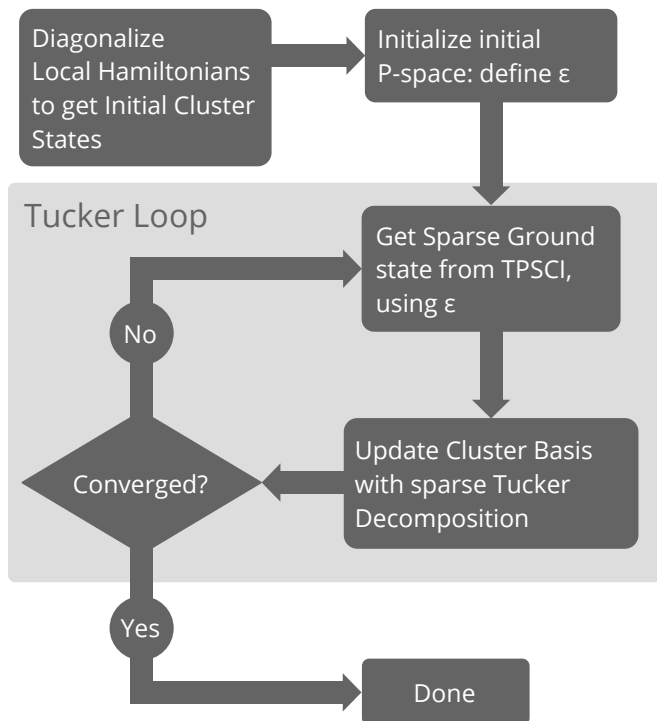


FIG. 2: Self consistent Tucker decomposition loop. After optimizing an approximate global state via TPSCI, the sparse tensor contraction can be easily used to perform a Tucker decomposition of the state. This involves diagonalizing the single cluster reduced density matrices. To retain local quantum numbers, we only block diagonalize the RDMs within a given Fock space. Because the Tucker decomposition often significantly decreases the number of variational parameters, one can optionally start with a loose threshold  $\epsilon_0$  to get a better set of cluster states, then tighten the threshold until it reaches the desired value,  $\epsilon$ , a procedure we refer to as “bootstrapping” explained in the Supplementary Information.

state basis to be the eigenvectors of the cluster’s reduced density matrix. For two clusters, this is of course equivalent to an SVD of the global state, or a MPS. When the number of clusters is greater than two, this generalizes to a higher-order SVD, or Tucker decomposition.<sup>30,36</sup>

In order to efficiently compute a cluster’s reduced density matrix,  $\rho_{IJ}$ , the contraction of the wavefunction over all other clusters needs to be possible.

$$\rho_{II'}^{N_\alpha^1, N_\beta^1} = c(I^{N_\alpha^1, N_\beta^1}, J^{N_\alpha^2, N_\beta^2}, \dots) c(I'^{N_\alpha^1, N_\beta^1}, J^{N_\alpha^2, N_\beta^2}, \dots) \quad (14)$$

Fortunately, only a few of these coefficients are non-zero due to the sparsity of the TPSCI approach, making the computation efficient. Once the cluster reduced density matrices are diagonalized, we repeat the TPSCI calculation to get a new global vector. This process is iterated until the density matrix stops changing, as illustrated in Fig. 2.

In the numerical simulations below, we find that the convergence is often quite quick such that the energy stops changing significantly after only a few iterations.

However, it is conceivable that this highly non-linear optimization could become a problem. In our previous work,<sup>36</sup> we found that a DIIS accelerated procedure which simultaneously extrapolates each cluster RDM greatly improved convergence in challenging cases. The same strategy could be applied here if needed.

### E. Implementation Details

One aspect of this work which is likely to impact performance is the mechanism chosen for storing the wavefunction. Since our states are sparse without any predictable structure in the indices, we simply choose to use a hash table to store the configurations. This is done using Python’s `OrderedDict` implementation. However, because we enforce local symmetries ( $\hat{N}$  and  $\hat{S}_z$ ), we use a nested hashmap. By specifying a Fock space configuration over  $n$  clusters as an immutable tuple-of-tuples  $((N_\alpha, N_\beta)_1, (N_\alpha, N_\beta)_2, \dots, (N_\alpha, N_\beta)_n)$  all TPS states with the same distribution of particle numbers can be described with a tuple of state indices:  $(I_1, J_2, \dots, K_n)$ . Consequently, an arbitrary TPS expansion coefficient can be accessed by two sequential hash table lookups:

$$\text{TBL2} = \text{TBL1}([(N_\alpha^1, N_\beta^1), (N_\alpha^2, N_\beta^2), \dots, (N_\alpha^n, N_\beta^n)]) \quad (15)$$

$$c(I^{N_\alpha^1, N_\beta^1}, J^{N_\alpha^2, N_\beta^2}, \dots, K^{N_\alpha^n, N_\beta^n}) = \text{TBL2}[I, J, \dots, K] \quad (16)$$

In addition to the storage and manipulation of the state vector information, storing the operator tensors from Eq. 11 also requires some care. Our code is organized in a class-based structure, such that each cluster is an instance of a `Cluster` class, which owns all local operator tensor data, stored as dense arrays. However, because we have preserved local symmetries, we can reduce the storage by keeping only the operator transitions which are not symmetry forbidden. As such, in order to access an operator tensor, we again use a hash table to map specific Fock space transitions to operator tensors. For example, consider two states, I and J, which live in Fock spaces  $(N_\alpha^I, N_\beta^I)$  and  $(N_\alpha^J, N_\beta^J)$ , respectively. The operator tensors associated with the  $\hat{p}^\dagger \hat{q}^\dagger \hat{r}$  operators only have data available if symmetry allowed, i.e., if  $N_\alpha^I == N_\alpha^J + 1$  and  $N_\beta^I == N_\beta^J$ . If that’s satisfied, then the dense tensor can be retrieved by a hash table lookup taking in the local Fock space transition:

$$\gamma_{pqr}^{IJ} = \text{DATA}[\text{string}(\text{AAa})][(N_\alpha^I, N_\beta^I, N_\alpha^J, N_\beta^J)] \quad (17)$$

where `string(AAa)` indicates a request for an operator string with three  $\alpha$  operators ( $A=\alpha, B=\beta$ ), and the first two are creation (upper case) and the last is annihilation (lower case). This allows us to have a fine grained control over the tensor contractions used to form matrix elements, preventing the computation of any hard zeros.

The key metric we focus on in this paper is accuracy vs number of parameters. While in the future our goal will also be to minimize CPU time, our initial implementation

has several limitations that greatly impact the computational efficiency. The most significant limitation is the lack of parallelization. As briefly mentioned above, each computationally intensive step of the TPSCI method is highly parallelizable. However, our current implementation, while still using BLAS<sup>37</sup> level tensor contractions via the `einsum` interface in NumPy,<sup>38</sup> uses Python as the main driver. This makes shared memory parallelization difficult. Although we are currently working on a new implementation to enable parallelization, this is not done yet, and as such, the computations take much more time than necessary.

A second limitation of our approach is a memory limitation due to the fact that the current code stores more data in memory than is necessary. In particular, we store all 1, 2, 3, and 4 index operator tensors for each cluster, in each Fock space. Clearly, the largest of these, the 4 index operator tensor, is local to a single cluster and could be handled separately without storage. This memory bottleneck prevents us from considering clusters larger than 6 orbitals. The size of this tensor,  $\gamma_{pqrs}^{I,J}$ , is  $\mathcal{O}(N^4 M^2)$  where  $M$  is the largest number of states in a Fock space, and  $N$  is the number of orbitals in the cluster. Because the number of states,  $M$ , increases factorially, it is difficult to store data for more than a few clusters having 6 orbitals. Future improvements to the code will involve manually handling these diagonal terms in a more memory efficient manner. Additionally, future work will investigate the efficiencies afforded by truncating the cluster state basis. The code can currently handle this, but we do not explore this in this paper for the purpose of minimizing the sources of errors in our analysis. Additional improvements can be made by manually handling the various tensor contractions. Currently these are handled in a rather abstract way which prevents much customization.

A third limitation restricts the size of the variational problem we can describe. This current implementation directly builds the full Hamiltonian in the  $\mathcal{P}$  space. This usually wasn't much of a bottleneck for most systems, as the TPSCI approach significantly reduces the size of the  $\mathcal{P}$  space. Nonetheless, improvements will be made in future work to replace the full Hamiltonian build with a direct matrix vector product to extend this to larger systems.

## F. Related works

There are several approaches in the literature which share the orbital clustering feature and TPS representation used in TPSCI. Perhaps the work most closely related to TPSCI is the Block Correlated Coupled Cluster (BCCC) approach of Li and coworkers.<sup>39-44</sup> In BCCC, the orbitals are grouped into clusters and the wavefunction is represented in a TPS basis. Then, inter-cluster correlations are treated with an exponential parameterization, whose amplitudes are solved for non-linearly. Our

method shares the TPS basis, but differs in both the treatment of intercluster correlation, and in the definition of the block states. Another cluster-based approach is the Renormalized Exciton Method (REM) of Malrieu and coworkers.<sup>45-48</sup> In contrast to both TPSCI and BCCC, REM includes the intercluster interactions via a Bloch effective Hamiltonian. In terms of the implementation, our approach is most closely related to the Active Space Decomposition (ASD) of Shiozaki and coworkers.<sup>49</sup> The ASD method was approximated to more than two clusters using a DMRG type wavefunction.<sup>50,51</sup> One can view TPSCI as a generalization of ASD to arbitrary numbers of clusters, with the global state optimization being approximated with CIPSI rather than the exact subspace diagonalization used in their work. Again, the Tucker decomposition basis is another distinguishing aspect of our current work. Another approach which helped inspire our current work is the Cluster Mean Field (cMF) method of Scuseria and coworkers.<sup>31</sup> CMF and TPSCI also share the orbital clustering, but TPSCI goes beyond the variational description of a single TPS, and again, the definition of the cluster states is different. Using cluster states to model excited states, the ab initio Frenkel Davydov Exciton Model (AIFDEM) of Herbert and coworkers approximate the low-lying singly excited states of aggregates using monomer direct product basis.<sup>52</sup>

Our TPSCI method also shares some features with other approaches which do not necessarily work with a TPS basis, but still involves some degree of orbital clustering. The ORMAS (occupation restricted multiple active space) method restricts the number of electrons in different orbital blocks and truncates the configuration expansion.<sup>53</sup> The Restricted Active-Space (RAS) method<sup>54</sup> and Generalized Active-Space method are also approaches which involve orbital clustering, but the similarities essentially end there.<sup>55</sup>

## III. RESULTS AND DISCUSSION

Our main focus in this paper will be a comparison between the TPSCI method and Slater determinant based SCI to understand how clustering impacts the compactness of the representation. In many of the results below, we use a simple convergence technique we refer to as “bootstrapping” which avoids going through larger parameter intermediate steps during the Tucker optimization. This approach is explained in the Supplementary Information.

For validating the TPSCI approach, we first explore a simple modified Hubbard model which allows us to manually tune the impact of “clusterability” on the performance of TPSCI. We then consider ab initio systems, and present data for N<sub>2</sub>, CO and HF bond dissociation curves and ground state energies for a few  $\pi$  conjugated systems. The SCI data quoted for the Hubbard model, HF molecule and the  $\pi$  conjugated systems were obtained using the PyScf<sup>56</sup> implementation of heat-bath CI.<sup>17</sup> For

$N_2$  and CO, the quoted SCI data was obtained using a simple local CIPSI implementation. The integrals for all the molecular examples were computed using PyScf. For systems without FCI results, we compare the TPSCI results to DMRG. The DMRG results were obtained using the ITensor library.<sup>57</sup>

### A. Hubbard Model

Model Hamiltonians provide a useful tool for exploring the behavior of different approximate models. In this section, we use the Hubbard model to explore how the inherent “clusterability” of a system of fermions affects the performance of TPSCI.

#### 1. Hubbard: Effect of Clusterability

Being motivated by the assumption that one can find some local structure in the Hamiltonian, the uniform Hubbard model is taken as our worst case scenario, and we expect our method to be inefficient in this domain. Since we are working in a TPS basis, the best case scenario would be a Hamiltonian with no interactions between clusters. In such a case, the exact ground state becomes a single TPS. We expect a wide variety of physical systems to occur between these artificial limits. As such, we start in Fig. 3(a) by exploring the transition between uniform lattice to a highly clusterable lattice, by scanning the relative strength of the Hamiltonian coupling between clusters. The Hamiltonian used has two distinct hopping terms, and one electron-electron repulsion term:

$$\hat{H} = \sum_{\langle i,j \in A \rangle \sigma} -t_1 c_{i\sigma}^\dagger c_{j\sigma} + \sum_{\langle i \in A, j \in B \rangle \sigma} -t_2 c_{i\sigma}^\dagger c_{j\sigma} + U \sum_j n_{i\uparrow} n_{j\downarrow} \quad (18)$$

where  $t_1$  ( $t_2$ ) denote hopping within (between) clusters, and  $U$  is the Coulomb repulsion. In order to make this a strongly correlated system, we set  $U = 5t_1$  and start with a uniform lattice,  $t_1 = t_2 = 1$ . We then change the magnitude of the inter-cluster hopping,  $t_2$ , scaled as  $\frac{t_1}{2^n}$  where  $n$  varies from 1 to 5.

In Fig. 3, we observe confirmation that the accuracy and compactness of TPSCI should increase with increasing clusterability. For this strongly correlated system, Slater determinant-based SCI (in this case HCI) was not able to find accurate results for any point on this scan, with reasonable numbers of variational parameters. Using Slater determinants, HCI uses approximately a million determinants and still does not achieve qualitative accuracy (Figure 3(b)). While accurate results can certainly be obtained with HCI, it will necessarily require many more variables than we have included in Fig. 3(c). While these results are consistent with our expectations,

we were surprised by the unexpected good performance of TPSCI for the worst case situation of a uniform lattice ( $t_1 = t_2$ ). In this case, TPSCI provided more accurate results with fewer parameters than HCI, despite the Hamiltonian not having any clusterable structure.

At lower ratios of  $t_1 : t_2$ , the TPSCI results are almost exact with a variational space of less than a few thousand configurations. This is a result of the fact that the exact ground state is moving increasingly close to a single TPS. Hence in the single particle basis, the representation is not really sparse and far more determinants than computationally feasible might need to be included for such an example.

#### 2. Hubbard: Effect of Lattice Size

In this second example, we study the effect on accuracy and dimension of variational space by increasing the size of the system. To do this, we fix the  $t_1/t_2$  ratio to  $\frac{1}{2}$ , a value which is somewhat clusterable yet challenging. Consistent with the previous section, we set  $U = 5t_1$ . We start with the 16-site problem from above, but now increase the system size from 16, to 36, to 64 site lattices. Based on the performance on the 16 site problem, we did not attempt to compute the HCI energies for these larger lattices. Also consistent with the above section, the TPSCI calculations uses a clustering in which all  $t_1$ -coupled sites form a cluster. As such, the three different systems have 4, 9, and 16 clusters, respectively. This is shown in Figure 4.

We compare these results with DMRG values with a fixed M value of 1600. We also plot the reference TPS energy for these systems for comparison. Despite this being a 2D systems, DMRG works quite well, although for the larger lattices (especially the 64 site lattice), the accuracy of TPSCI approaches that of DMRG. We note though, that it’s difficult to achieve a fair comparison of TPSCI and DMRG, as both can be systematically improved to get arbitrarily accurate results. Nonetheless, for the 64-site example, the variational energy for TPSCI (using 1248 variables) is better than the DMRG result using M=1600. Of course with our unoptimized code, the DMRG calculation took significantly less time than the TPSCI result, but we anticipate significant efficiency improvements in future work.

One challenge arises when studying the Hubbard model with different Hamiltonian parameters. Because the Hamiltonian enters into the selection criterion for the TPSCI method (via the first order amplitudes), we find that the TPSCI threshold value  $\epsilon$  does not yield consistent convergence behavior. This means that the accuracy of the method cannot be directly linked to the selection criteria when modeling different Hamiltonians. While we only notice this problem with the Hubbard Hamiltonian, it is something we plan to investigate more in the future. One strategy would be to develop a TPSCI version of the  $\Lambda$ -CI method of Evangelista for growing the  $\mathcal{P}$  space.<sup>24</sup>

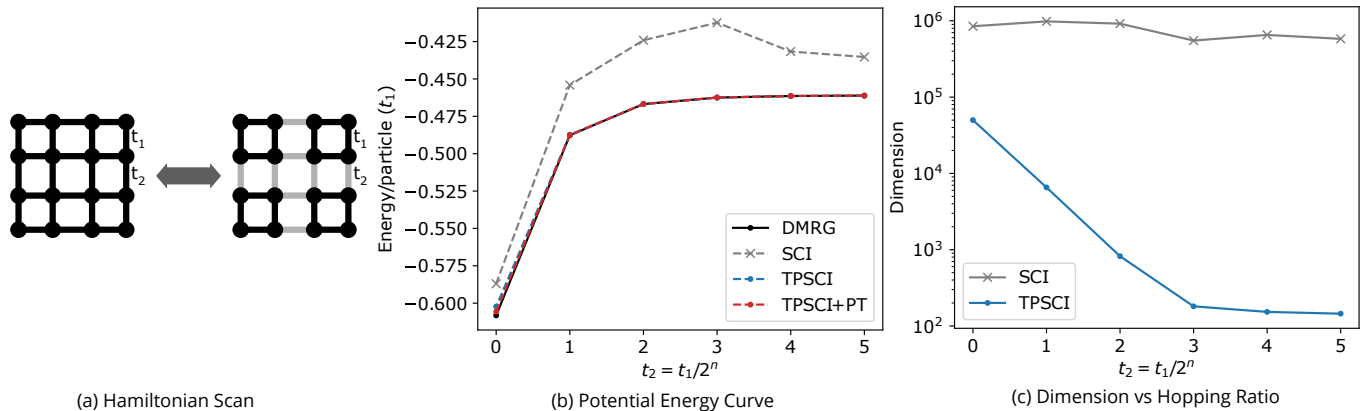


FIG. 3: Clusterability of the Hubbard model. (a) Schematic representation of the Hubbard model used for the data, dark lines correspond to  $t_1$  and lighter lines correspond to  $t_2$ . (b) Energy/site of the system as the  $t_1 : t_2$  ratio is changed. (c) Comparison of the dimension of the variational space as the  $t_1 : t_2$  ratio is changed. DMRG result uses  $M=1600$ . SCI in this case indicates Heat-bath CI.

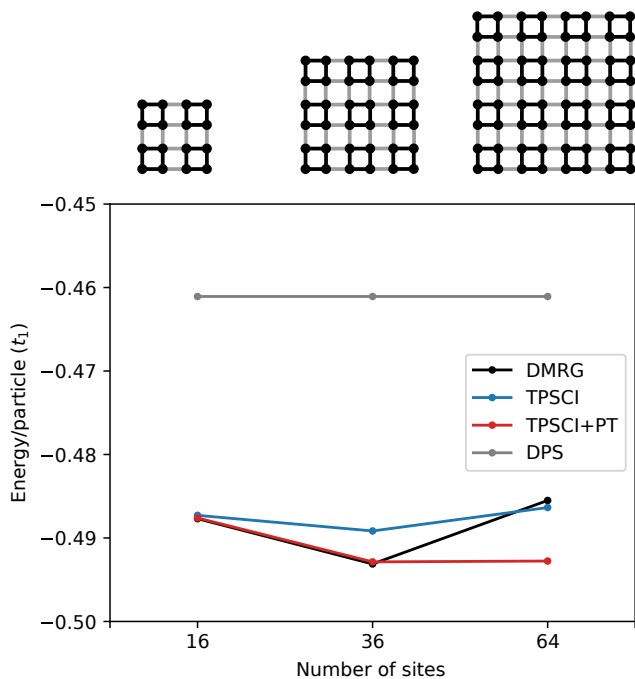


FIG. 4: Size dependence of the Hubbard model. Energy/particle vs lattice size. Intra-cluster:Inter-cluster hopping ratio = 2:1. TPSCI dimensions for each data point: 16-site: 6552, 36-site: 6189, 64-site: 1269

which is designed to have better accuracy guarantees.

## B. Nitrogen Molecule

While model Hamiltonians are useful for artificially exploring the behavior of an approximation, the ultimate

goal of our work is to produce an efficient method for ab initio molecular simulation. To understand the behavior for molecular electronic structure, we start with a canonical example of a small strongly correlated system:  $N_2$  dissociation.

For the Hubbard model it was straightforward to form the clusters based on sparsity of the hopping term. In contrast, for molecular systems the clustering can be far from straightforward. For example, the orbitals in  $N_2$  could reasonably be clustered based on two different obvious criteria: one based on maximizing localization, and one based on chemical bonding intuition. The straightforward way to do this using localization is to first localize the orbitals and assign them to clusters based on atomic centers (i.e orbitals localized on N1 belong to one cluster and those on N2 belong in another cluster). Alternatively, by ensuring that bonding and antibonding pairs are contained in the same cluster, one might arrive at a very different clustering, one similar to a perfect pairing model type clustering.<sup>58,59</sup> We explore both of these choices in Figures 5 and 6, respectively.

### 1. $N_2$ : Clustering based on localization

For local orbitals, the clusters are defined to be comprised of orbitals on each atom. In a minimal basis with frozen 1s orbitals, there are two clusters (N1,N2) each with four orbitals ( $2s, 2p_x, 2p_y, 2p_z$ ) in each cluster. The localized orbitals were obtained using the Boys-Foster<sup>60</sup> localization algorithm among the active orbitals. The orbitals corresponding to each cluster are shown in Figure 5(a). This clustering would clearly lead to a very good result at the dissociation limit, but at shorter distances, the clustering is less efficient.

In order to demonstrate the impact of the Tucker op-



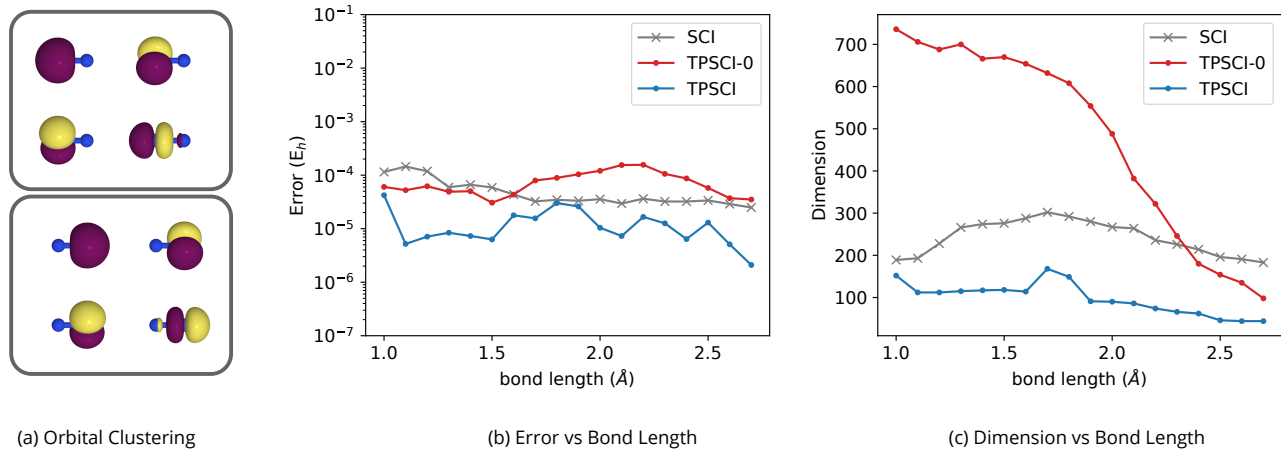


FIG. 5: Nitrogen molecule with clustering based on localized orbitals. Comparisons are made between TPSCI, the Slater determinant-based CIPSI (SCI), and TPSCI but without any Tucker optimization (labelled with TPSCI-0). (a) The two clusters defined using the localized orbitals for N<sub>2</sub> molecule (b) Error from CAS-CI results for the initial TPSCI, TPSCI-0, and SCI method (c) Dimension of the variational space along the PES scan.

timization, we compare the converged TPSCI results to the TPSCI method using the fixed local eigenstates to define the cluster basis (TPSCI-0). To compare TPSCI, TPSCI-0, and Slater determinant CIPSI, we converge each method to a similar accuracy, shown in Figure 5(b). From Figure 5(c), it can be seen that at short distances the TPSCI-0 needs a larger variational space than even CIPSI. This is a result of the fact that the eigenbasis of atomic nitrogen is a poor basis for N<sub>2</sub>. In comparison, the Tucker decomposition leads to a much more compact representation with a significantly reduced error. The cluster reduced density matrix diagonalization (Tucker decomposition) compresses the variational space by a large factor and the total number of configurations in the final wavefunction is less than that for the traditional SCI method for these systems.

## 2. N<sub>2</sub>: Clustering based on bonding

Instead of trying to force N<sub>2</sub> into a localized basis, one could instead consider the bonding characteristics when choosing a clustering. N<sub>2</sub> is triply bonded with one  $\sigma$  and two  $\pi$  type bonds. The  $2s$  and  $2p_z$  orbitals in each atom mix and form hybridized orbitals. These orbitals form the  $\sigma$  bond, and the  $2p_x$  and  $2p_y$  form the two  $\pi$  bonds. If no inter-bond correlations occurred, the exact solution would then be a single TPS. Of course, inter-bond correlations do exist, but we can use this as a starting point to define a qualitatively correct TPS reference for TPSCI. Because the TPSCI approach is flexible for arbitrary clusterings, we can also explore the grouping of different bonds together. The different clusterings we considered are as follows:

- 4c:  $(2s\sigma, 2s\sigma^*), (\sigma_z, \sigma_z^*), (\pi_x, \pi_x^*), (\pi_y, \pi_y^*)$

- 3c:  $(2s\sigma, 2s\sigma^*, \sigma_z, \sigma_z^*), (\pi_x, \pi_x^*), (\pi_y, \pi_y^*)$
- 2c:  $(2s\sigma, 2s\sigma^*, \sigma_z, \sigma_z^*), (\pi_x, \pi_x^*, \pi_y, \pi_y^*)$

These results are displayed in Figure 6.

Intuitively, we find that the accuracy/dimension is more favorable when more correlations are included inside of a cluster. By comparing the 2c and 3c results, one can see the dramatic effect of including the  $2s$  orbitals alongside the  $2p_z$  inside the same cluster. Further improvement is then made by combining the two  $\pi$  bond/antibond pairs. Comparing the 2c results in Figure 6 to the results in Figure 5, we observe that the bond pattern based clustering has a significant advantage over the localization based clustering for this system. However, we don't expect this to be true for all systems, and we plan on exploring systems in future work to better understand this behavior. Additionally, due to the compactness of this partitioning, an interesting direction to take in future work is to do TPSCI using perfect-pairing orbitals instead of RHF orbitals.

## C. Carbon Monoxide

Being isoelectronic to N<sub>2</sub>, but with a dipole moment, carbon monoxide allows us to explore how atomic number can affect the results. For this system we use RHF orbitals and cluster based on bonding, similar to the 2c clustering in N<sub>2</sub>. We partition the system into two clusters such that the  $\pi$  bonding orbitals ( $\pi_x, \pi_x^*, \pi_x$  and  $\pi_x^*$ ) are in a cluster and the  $\sigma$  bonding orbitals ( $2s\sigma, 2s\sigma^*, \sigma_z, \sigma_z^*$ ) are in another cluster.

From Figure 7(c), we can see that the TPSCI wavefunction is very compact compared to the traditional SCI method. The improvement of TPSCI over CIPSI is even

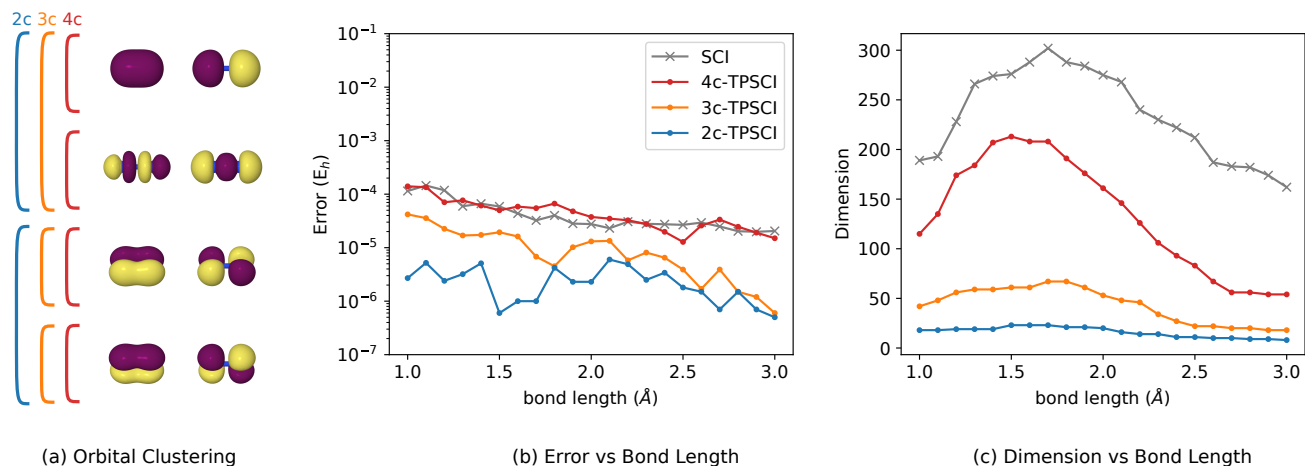


FIG. 6: Nitrogen molecule with clustering based on bonding patterns. (a) The molecular orbitals for  $N_2$  and the clustering choices (2c) two clusters, (3c) three clusters and (4c) four clusters (b) Error with CAS-CI results for TPSCI method with the three different clustering options (c) dimension of the variational space along the PES scan

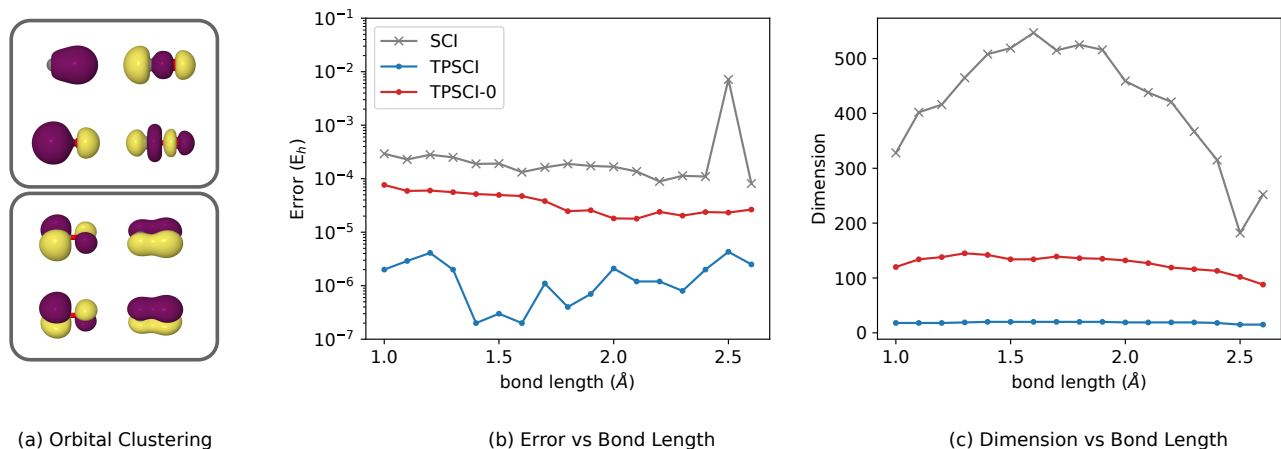


FIG. 7: Carbon monoxide with clustering based on bonding patterns. Comparisons are made between TPSCI, the Slater determinant-based CIPSI (labelled SCI), and TPSCI, but without any Tucker optimization (labelled with TPSCI-0). (a) The molecular orbitals of CO put into two clusters (b) Error from CAS-CI results for the initial TPSCI, TPSCI-0, and SCI method (c) Dimension of the variational space along the PES scan

more pronounced here than in  $N_2$ , with both the dimension and error being significantly reduced. For the CO molecule, we also plot the error and variational dimension of the TPSCI-0 method to compare with the TPSCI method. Similar to the  $N_2$  case, we see that the Tucker basis leads to a much more compact wavefunction when compared to the TPSCI-0 results.

#### D. Hydrogen Fluoride at ccpvdz

So far only minimal basis set results have been considered. While this makes clustering more straightforward, and allowed us to focus solely on static correlation, it's

not obvious that the same advantages transfer to systems with dynamical correlation as well. To investigate the effect of dynamical correlation on the performance of TPSCI, in Figure 8 we provide results for hydrogen fluoride in the ccpvdz basis. After freezing the core 1s orbital on F, the active space has 18 orbitals and 8 electrons. Although this has significantly more orbitals, the relatively small number of electrons means that we can still compare to FCI. Increasing the basis set can make finding an efficient clustering less obvious. There are 8  $A_1$  symmetry orbitals, mainly formed using linear combinations of s and  $p_z$  orbitals. We again cluster this system similar to the bonding-antibonding clustering, but by including more orbitals with same symmetry as before into

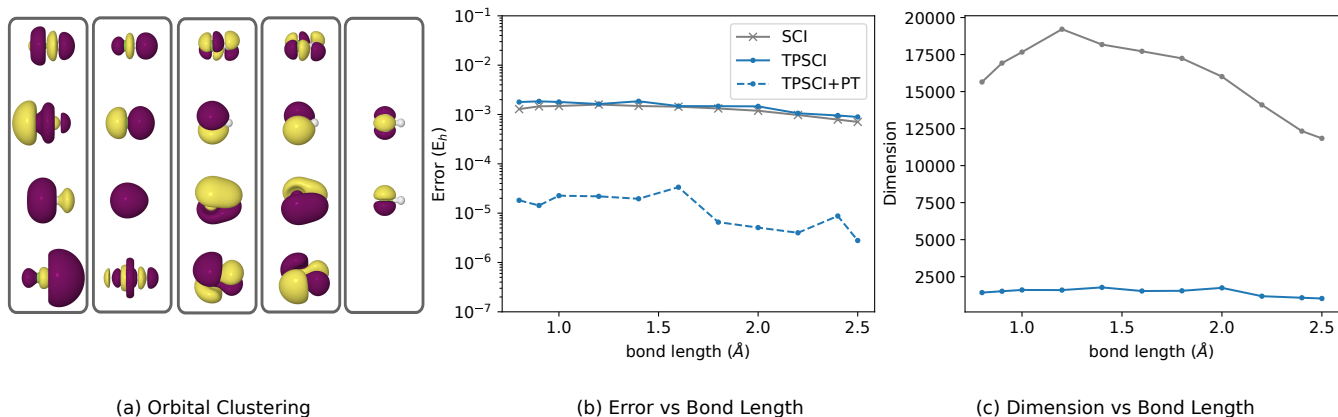


FIG. 8: Hydrogen Fluoride molecule with ccpvdz basis. (a) The molecular orbital clustering of HF at 1.0 Å. (b) Error from CAS-CI results for TPSCI with HCI. (c) Dimension of the variational space along the PES scan.

the same cluster. We partition the full system into 5 clusters as explained below in Figure 8(a). Since there are 8 orbitals with A1 symmetry and storing the operator tensors from Eq. 11 for an 8-site cluster is beyond our programs current memory constraints (as discussed in the Implementation Details section), we partition that into two clusters. We also have clusters formed using E1x (4 orbitals), E1y (4 orbitals) and E2 (2 orbitals) symmetry.

We present the error compared to FCI results along the PES scan in Figure 8(b). We converge both TPSCI and HCI to a similar accuracy level. An initial observation is that the errors do not fluctuate significantly along the PES for both HCI and TPSCI method. When comparing the number of configurations between the two methods, it can be seen that the TPSCI method only has 10% of the variational space as compared to HCI and gives similar accuracy. The PT correction gives further accurate results with errors in the range of  $10^{-5}$  Hartrees and perturbation theory corrections could also be applied to HCI, as has been done by Sharma and coworkers.<sup>26</sup> The fact that the errors do not vary much is primarily due to the clustering. By choosing the cluster in a bonding-antibonding orbitals fashion, the interaction changes most within each cluster rather than between the cluster as the molecule dissociates. Because the intra-cluster interactions are modeled at a higher level of theory, TPSCI is able to capture this correlation well if the clusters are properly chosen. This data suggests that TPSCI might be a promising method for studying systems with both static and dynamic correlations.

#### E. $\pi$ -conjugated system

Moving to larger systems, we now investigate the behavior of TPSCI for computing the ground state of  $\pi$ -conjugated systems.<sup>61</sup> Previous cluster based ap-

proaches have been used to study dimer or trimer systems where the clustering does not disrupt the delocalized  $\pi$  system.<sup>32,51</sup> By breaking the  $\pi$  system, the electron delocalization is limited, disrupting the long-range electronic structure. We find this to be an interesting test case to push the boundaries of the TPSCI approach. In Figure 9(a), we report TPSCI results obtained by partitioning several strongly interacting  $\pi$  conjugated systems, including: naphthalene, 1,3,5-trivinylbenzene, and two trans-linear-n-polyacetylene molecules ( $n=4,6$ ).

For each of the molecules, an active space is formed from the localized  $2p_z$  orbital basis. The HCI results were instead obtained using canonical orbitals. The partitioning of the molecule to form clusters is represented by blue dotted lines in Figure 9. For 1,3,5-trivinylbenzene (**3**), note that the fragments partition the delocalized benzene ring into 3 clusters and still achieve quite accurate results with a compact wavefunction. Although better clustering options for this molecule may exist, this particular clustering has been chosen to show that the TPSCI algorithm is able to include important configurations to form a compact wavefunction even when the coefficient of the dominant configuration is relatively small (only .62). Techniques of finding the best orbital clusterings will be left for future work. Naphthalene is partitioned into 3 clusters and also achieves good performance. In each case in Figure 9(b)/(c), the error for TPSCI is below chemical accuracy (and SCI) while still being much more compact as compared to that of SCI.

#### IV. CONCLUSION AND FUTURE WORK

In this work, we have introduced a new selected CI method using tensor products of cluster states as the basis. By folding the most important correlations into the basis vectors themselves, much more compact wavefunc-

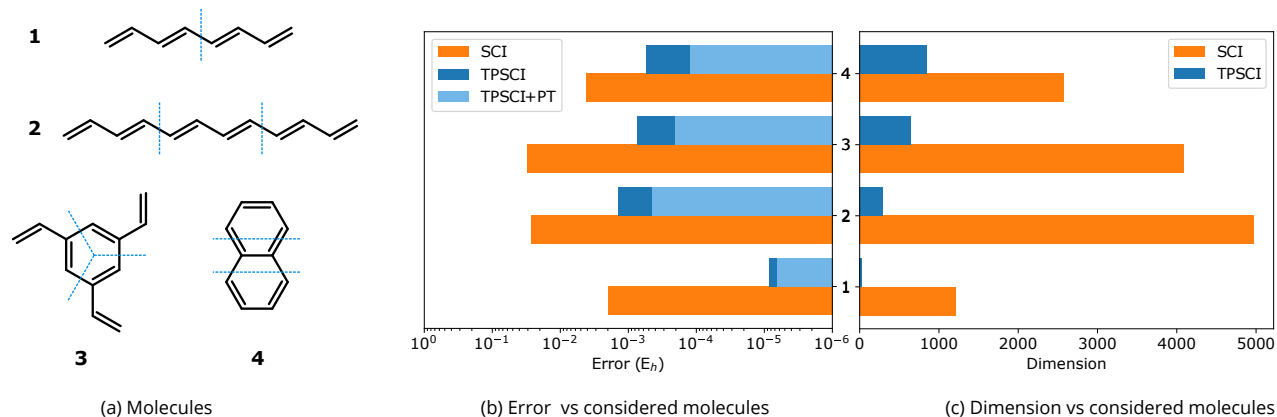


FIG. 9:  $\pi$ -conjugated systems. (a) The molecules considered (b) Error in Hartree for each of the molecules in (a) (c) Dimension of the variational space.

tions can be obtained using the basic selected CI procedures, a feature which significantly improves the performance for strongly correlated systems. In choosing the nature of the cluster states, we found that the Tucker decomposition provided a simple and efficient way to significantly improve the compactness of the final TPSCI wavefunction.

This initial paper presents the algorithm, an implementation, and proof of concept results. However, much work remains to be done. A few of the ongoing and future works will involve:

1. Exploring the performance of cluster basis truncation. By including only a subset of the cluster states on a cluster, we can use larger clusterings which should converge even faster. However, the key question is how to determine which states to discard at the beginning? We are currently working on this question, and have found that using a cluster mean field<sup>31</sup> starting point, significantly reduces the truncation error, but this work is still underway.
2. Improved implementation. While our current code is efficient enough to obtain all the results in this manuscript, including the 64 site Hubbard lattice example, calculations with ab initio Hamiltonians are much slower than necessary due to a lack of any parallelization. This, along with the memory usage limitations discussed in the Theory section, will be improved in future work.
3. Exploring how the different components of the various SCI methods such as HCI, ACI, ASCI, etc. behave in the TPS basis.
4. Extending the method to study excited states. One possible route would be to use similar approach

taken in the original CIPSI work. Another interesting direction is to form a reference state using single excitations in clusters as done in AIFDEM<sup>62</sup> and include important configurations avoiding collapse to the ground state.

## V. ACKNOWLEDGEMENTS

This research was supported by the National Science Foundation (Award No. 1752612).

## References

- \* Electronic address: nmayhall@vt.edu
- 1 White, S. R. Density matrix formulation for quantum renormalization groups. *Phys. Rev. Lett.* **1992**, *69*, 2863–2866.
  - 2 Schollwöck, U. The density-matrix renormalization group. *Rev. Mod. Phys.* **2005**, *77*, 259–315.
  - 3 Chan, G. K.-L.; Sharma, S. The density matrix renormalization group in quantum chemistry. *Ann. Rev. Phys. Chem.* **2011**, *62*, 465–81.
  - 4 Jordan, J.; Orús, R.; Vidal, G.; Verstraete, F.; Cirac, J. I. Classical Simulation of Infinite-Size Quantum Lattice Systems in Two Spatial Dimensions. *Phys. Rev. Lett.* **2008**, *101*, 250602.
  - 5 Verstraete, F.; Cirac, J. I. Renormalization Algorithms for Quantum-Many Body Systems in Two and Higher Dimensions. *arXiv:cond-mat/0407066* **2004**,
  - 6 Hyatt, K.; Stoudenmire, E. M. DMRG Approach to Optimizing Two-Dimensional Tensor Networks. *arXiv:1908.08833 [cond-mat, physics:quant-ph]* **2019**,
  - 7 Kovyrshin, A.; Reiher, M. Self-adaptive tensor network states with multi-site correlators. *The Journal of Chemical Physics* **2017**, *147*, 214111.
  - 8 Marti, K. H.; Bauer, B.; Reiher, M.; Troyer, M.; Verstraete, F. Complete-Graph Tensor Network States: A

- New Fermionic Wave Function Ansatz for Molecules. *New Journal of Physics* **2010**, *12*, 103008–103008.
- <sup>9</sup> Murg, V.; Verstraete, F.; Schneider, R.; Nagy, P. R.; Legeza, O. Tree Tensor Network State with Variable Tensor Order: An Efficient Multireference Method for Strongly Correlated Systems. *Journal of Chemical Theory and Computation* **2015**, *11*, 1027–1036.
  - <sup>10</sup> Szalay, S.; Pfeffer, M.; Murg, V.; Barcza, G.; Verstraete, F.; Schneider, R.; Legeza, r. Tensor Product Methods and Entanglement Optimization for Ab Initio Quantum Chemistry. *International Journal of Quantum Chemistry* **2015**, *115*, 1342–1391.
  - <sup>11</sup> Choo, K.; Mezzacapo, A.; Carleo, G. Fermionic Neural-Network States for Ab-Initio Electronic Structure. *arXiv:1909.12852 [cond-mat, physics:physics, physics:quant-ph]* **2019**,
  - <sup>12</sup> Huron, B.; Malrieu, J. P.; Rancurel, P. Iterative perturbation calculations of ground and excited state energies from multiconfigurational zeroth-order wavefunctions. *J. Chem. Phys.* **1973**, *58*, 5745.
  - <sup>13</sup> Bender, C. F.; Davidson, E. R. Studies in Configuration Interaction: The First-Row Diatomic Hydrides. *Phys. Rev.* **1969**, *183*, 23–30.
  - <sup>14</sup> Buenker, R. J. Ab Initio SCF MO and CI Studies of the Electronic States of Butadiene. *J. Chem. Phys.* **1968**, *49*, 5381.
  - <sup>15</sup> Tubman, N. M.; Lee, J.; Takeshita, T. Y.; Head-Gordon, M.; Whaley, K. B. A deterministic alternative to the full configuration interaction quantum Monte Carlo method. *The Journal of Chemical Physics* **2016**, *145*, 044112.
  - <sup>16</sup> Schriber, J. B.; Evangelista, F. A. Communication: An adaptive configuration interaction approach for strongly correlated electrons with tunable accuracy. *The Journal of Chemical Physics* **2016**, *144*, 161106.
  - <sup>17</sup> Holmes, A. A.; Tubman, N. M.; Umrigar, C. J. Heat-Bath Configuration Interaction: An Efficient Selected Configuration Interaction Algorithm Inspired by Heat-Bath Sampling. *Journal of Chemical Theory and Computation* **2016**, *12*, 3674–3680.
  - <sup>18</sup> Liu, W.; Hoffmann, M. R. iCI: iterative CI toward full CI. *J. Chem. Theory Comput.* **2016**, *12*, 1169–1178.
  - <sup>19</sup> Chakraborty, R.; Ghosh, P.; Ghosh, D. Evolutionary algorithm based configuration interaction approach. *Int. J. Quantum Chem.* **2018**, *118*, e25509.
  - <sup>20</sup> Ohtsuka, Y.; Hasegawa, J.-y. Selected configuration interaction method using sampled first-order corrections to wave functions. *J. Chem. Phys.* **2017**, *147*, 34102.
  - <sup>21</sup> Coe, J. P. Machine Learning Configuration Interaction. *J. Chem. Theory Comput.* **2018**, *14*, 5739–5749.
  - <sup>22</sup> Booth, G. H.; Thom, A. J. W.; Alavi, A. Fermion Monte Carlo without fixed nodes: A game of life, death, and annihilation in Slater determinant space. *J. Chem. Phys.* **2009**, *131*, 54106.
  - <sup>23</sup> Cleland, D.; Booth, G. H.; Alavi, A. Communications: Survival of the fittest: Accelerating convergence in full configuration-interaction quantum Monte Carlo. *J. Chem. Phys.* **2010**, *132*, 41103.
  - <sup>24</sup> Evangelista, F. A. Adaptive multiconfigurational wave functions. *J. Chem. Phys.* **2014**, *140*, 124114.
  - <sup>25</sup> Holmes, A. A.; Changlani, H. J.; Umrigar, C. J. Efficient Heat-Bath Sampling in Fock Space. *J. Chem. Theory Comput.* **2016**, *12*, 1561–1571.
  - <sup>26</sup> Sharma, S.; Holmes, A. A.; Jeanmairet, G.; Alavi, A.; Umrigar, C. J. Semistochastic Heat-Bath Configuration Interaction Method: Selected Configuration Interaction with Semistochastic Perturbation Theory. *J. Chem. Theory Comput.* **2017**, *13*, 1595–1604.
  - <sup>27</sup> Smith, J. E. T.; Mussard, B.; Holmes, A. A.; Sharma, S. Cheap and Near Exact CASSCF with Large Active Spaces. *Journal of Chemical Theory and Computation* **2017**, *13*, 5468–5478.
  - <sup>28</sup> Greer, J. C. Estimating full configuration interaction limits from a Monte Carlo selection of the expansion space. *J. Chem. Phys.* **1995**, *103*, 1821–1828.
  - <sup>29</sup> Coe, J. P.; Paterson, M. J. Development of Monte Carlo configuration interaction: Natural orbitals and second-order perturbation theory. *J. Chem. Phys.* **2012**, *137*, 204108.
  - <sup>30</sup> Tucker, L. R. Some Mathematical Notes on Three-Mode Factor Analysis. *Psychometrika* **1966**, *31*, 279–311.
  - <sup>31</sup> Jiménez-Hoyos, C. A.; Scuseria, G. E. Cluster-based mean-field and perturbative description of strongly correlated fermion systems: Application to the one- and two-dimensional Hubbard model. *Phys. Rev. B* **2015**, *92*, 085101.
  - <sup>32</sup> Parker, S. M.; Shiozaki, T. Communication: Active Space Decomposition with Multiple Sites: Density Matrix Renormalization Group Algorithm. *The Journal of chemical physics* **2014**, *141*, 211102–211102.
  - <sup>33</sup> Parker, S. M.; Seideman, T.; Ratner, M. A.; Shiozaki, T. Communication: Active-Space Decomposition for Molecular Dimers. *J. Chem. Phys.* **2013**, *139*, 021108.
  - <sup>34</sup> Epstein, P. S. The Stark Effect from the Point of View of Schroedinger’s Quantum Theory. *Physical Review* **1926**, *28*, 695–710.
  - <sup>35</sup> Nesbet, R. K.; Hartree, D. R. Configuration interaction in orbital theories. *Proceedings of the Royal Society of London. Series A. Mathematical and Physical Sciences* **1955**, *230*, 312–321.
  - <sup>36</sup> Mayhall, N. J. Using Higher-Order Singular Value Decomposition To Define Weakly Coupled and Strongly Correlated Clusters: The n -Body Tucker Approximation. *J. Chem. Theory Comput.* **2017**, *13*, 4818–4828.
  - <sup>37</sup> Blackford, L. S.; Demmel, J.; Dongarra, J.; Duff, I.; Hammarling, S.; Henry, G.; Heroux, M.; Kaufman, L.; Lumsdaine, A.; Petitet, A.; Pozo, R.; Remington, K.; Whaley, R. C. An Updated Set of Basic Linear Algebra Subprograms (BLAS). *ACM Transactions on Mathematical Software* **2001**, *28*, 135–151.
  - <sup>38</sup> van der Walt, S.; Colbert, S. C.; Varoquaux, G. The NumPy Array: A Structure for Efficient Numerical Computation. *Computing in Science Engineering* **2011**, *13*, 22–30.
  - <sup>39</sup> Fang, T.; Li, S. Block Correlated Coupled Cluster Theory with a Complete Active-Space Self-Consistent-Field Reference Function: The Formulation and Test Applications for Single Bond Breaking. *The Journal of Chemical Physics* **2007**, *127*, 204108–204108.
  - <sup>40</sup> Fang, T.; Shen, J.; Li, S. Block Correlated Coupled Cluster Method with a Complete-Active-Space Self-Consistent-Field Reference Function: The Implementation for Low-Lying Excited States. *The Journal of Chemical Physics* **2008**, *129*, 234106–234106.
  - <sup>41</sup> Fang, T.; Shen, J.; Li, S. Block Correlated Coupled Cluster Method with a Complete-Active-Space Self-Consistent-Field Reference Function: The Formula for General Active Spaces and Its Applications for Multibond Break-

- ing Systems. *The Journal of Chemical Physics* **2008**, *128*, 224107–224107.
- <sup>42</sup> Li, S. Block-Correlated Coupled Cluster Theory: The General Formulation and Its Application to the Antiferromagnetic Heisenberg Model. *The Journal of Chemical Physics* **2004**, *120*, 5017–5017.
- <sup>43</sup> Shen, J.; Li, S. Block Correlated Coupled Cluster Method with the Complete Active-Space Self-Consistent-Field Reference Function: Applications for Low-Lying Electronic Excited States. *Journal of Chemical Physics* **2009**, *131*.
- <sup>44</sup> Xu, E.; Li, S. Block Correlated Second Order Perturbation Theory with a Generalized Valence Bond Reference Function. *The Journal of Chemical Physics* **2013**, *139*, 174111–174111.
- <sup>45</sup> Al Hajj, M.; Malrieu, J.-P.; Guihéry, N. Renormalized excitonic method in terms of block excitations: Application to spin lattices. *Phys. Rev. B* **2005**, *72*, 224412.
- <sup>46</sup> Zhang, H.; Malrieu, J.-P.; Ma, H.; Ma, J. Implementation of renormalized excitonic method at ab initio level. *J. Comput. Chem.* **2011**, *33*, 34–43.
- <sup>47</sup> Ma, Y.; Liu, Y.; Ma, H. A new fragment-based approach for calculating electronic excitation energies of large systems. *J. Chem. Phys.* **2012**, *136*, 024113.
- <sup>48</sup> Ma, Y.; Ma, H. Calculating excited states of molecular aggregates by the renormalized excitonic method. *J. Phys. Chem. A* **2013**, *117*, 3655–3665.
- <sup>49</sup> Parker, S. M.; Seideman, T.; Ratner, M. A.; Shiozaki, T. Communication: Active-space decomposition for molecular dimers. *J. Chem. Phys.* **2013**, *139*, 021108.
- <sup>50</sup> Parker, S. M.; Seideman, T.; Ratner, M. A.; Shiozaki, T. Model Hamiltonian Analysis of Singlet Fission from First Principles. *J. Phys. Chem. C* **2014**, *118*, 12700–12705.
- <sup>51</sup> Nishio, S.; Kurashige, Y. Rank-one basis made from matrix-product states for a low-rank approximation of molecular aggregates. *The Journal of Chemical Physics* **2019**, *151*, 084110.
- <sup>52</sup> Morrison, A. F.; You, Z.-Q.; Herbert, J. M. Ab Initio Implementation of the Frenkel-Davydov Exciton Model: A Naturally Parallelizable Approach to Computing Collective Excitations in Crystals and Aggregates. *J. Chem. Theory Comput.* **2014**, *10*, 5366–76.
- <sup>53</sup> Ivanic, J. Direct configuration interaction and multiconfigurational self-consistent-field method for multiple active spaces with variable occupations. I. Method. *J. Chem. Phys.* **2003**, *119*, 9364.
- <sup>54</sup> Olsen, J.; Roos, B. O.; Jorgensen, P.; Jensen, H. J. A. Determinant based configuration interaction algorithms for complete and restricted configuration interaction spaces. *J. Chem. Phys.* **1988**, *89*, 2185.
- <sup>55</sup> Ma, D.; Li Manni, G.; Gagliardi, L. The generalized active space concept in multiconfigurational self-consistent field methods. *J. Chem. Phys.* **2011**, *135*, 044128.
- <sup>56</sup> Sun, Q.; Berkelbach, T. C.; Blunt, N. S.; Booth, G. H.; Guo, S.; Li, Z.; Liu, J.; McClain, J. D.; Sayfutyarova, E. R.; Sharma, S.; Wouters, S.; Chan, G. K.-L. PySCF: the Python-based simulations of chemistry framework. *WIREs Computational Molecular Science* **2018**, *8*, e1340.
- <sup>57</sup> *ITensor Library (version 2.0.11)* <http://itensor.org>
- <sup>58</sup> Hunt, W.; Hay, P.; Goddard Iii, W. Self-Consistent Procedures for Generalized Valence Bond Wavefunctions. Applications H3, BH, H2O, C2H6, and O2. *The Journal of Chemical Physics* **1972**, *57*, 738–748.
- <sup>59</sup> Beran, G. J. O.; Austin, B.; Sodt, A.; Head-Gordon, M. Unrestricted Perfect Pairing: The Simplest Wave-Function-Based Model Chemistry beyond Mean Field. *The Journal of Physical Chemistry A* **2005**, *109*, 9183–9192, PMID: 16332028.
- <sup>60</sup> Boys, S. Construction of Some Molecular Orbitals to Be Approximately Invariant for Changes from One Molecule to Another. *Rev. Mod. Phys.* **1960**, *32*, 296–299.
- <sup>61</sup> Milin-Medina, B.; Gierschner, J. Conjugation. *WIREs Computational Molecular Science* **2012**, *2*, 513–524.
- <sup>62</sup> Morrison, A. F.; Herbert, J. M. Evidence for Singlet Fission Driven by Vibronic Coherence in Crystalline Tetracene. *J. Phys. Chem. Lett.* **2017**, *8*, 1442–1448.